Research Article

Received: 11 February 2024 Revised: 19 April 2024 Published online in Wiley Online Library: 3 June 2024

(wileyonlinelibrary.com) DOI 10.1002/pi.6667

Sustainable biomaterials for tissue engineering: electrospun polycaprolactone fibers enriched with freshwater snail calcium carbonate and waste human hair keratin

Özge Erdemli,[a*] Bengi Yilmaz,[b] İrem Göksu Saran[a] and Erdal Serin[b]

Abstract

This study focuses on developing a sustainable and biocompatible polycaprolactone (PCL)-based scaffold for bone tissue engineering through electrospinning, utilizing calcium carbonate ($CaCO_3$) from *Pomacea canaliculata* shells and keratin from human hair, known for stimulating bone regeneration. The isolated $CaCO_3$ has been identified to demonstrate two polymorphs, vaterite and calcite, as determined by X-ray diffraction. The isolation of keratin from human hair was confirmed through sodium dodecyl sulfate polyacrylamide gel electrophoresis and Fourier transform infrared spectroscopy analysis, revealing the presence of α-keratin structures around 45–50 kDa and β-keratin structures around 55–60 kDa. According to scanning electron microscope observations, the addition of keratin to PCL fibers reduced their diameter from 457 $\pm$ 345 to 371 $\pm$ 103 nm. Further addition of calcium carbonate led to a mean diameter of 258 $\pm$ 76 nm. The melting temperature of PCL fibers containing keratin and $CaCO_3$ was determined to be 76.17 °C via differential scanning calorimetry, while thermogravimetric analysis, conducted at temperatures up to 600 °C, revealed a remaining ash content of 9.59%. Calcium phosphate accumulation was observed to initiate on PCL fibers containing keratin and $CaCO_3$ following a 7-day exposure to simulated body fluid. The fibers exhibit cytocompatibility, showing no toxicity while supporting the growth and proliferation of Saos-2 osteosarcoma cells. The results suggest that the innovative incorporation of keratin and $CaCO_3$ into PCL nanofibers could serve as a bioactive matrix compared to pure PCL matrices, thereby offering enhanced potential for bone tissue engineering applications.

Keywords: keratin; calcium carbonate; polycaprolactone (PCL); electrospinning; bone scaffold

INTRODUCTION

In recent years, there has been a growing interest in the development of bone tissue engineering strategies that utilize natural and sustainable sources instead of relying solely on synthetic materials. Natural materials offer excellent biocompatibility, minimizing the risk of adverse reactions and facilitating seamless integration with the body, often possess inherent bioactive properties and they can closely mimic the composition and structure of native tissues.[1,2] Sustainability is another crucial consideration, as using renewable sources reduces reliance on synthetic materials and the acceptance of natural materials by regulatory agencies facilitates clinical translation, expediting the application of innovative techniques in patient care. Collectively, these factors drive the exploration and development of natural and sustainable approaches in bone tissue engineering, ultimately improving patient outcomes.

Keratin is a cysteine-rich fibrous protein derived from hair, wool, horns, nails, claws and hooves of mammals and feathers, beaks and claws of birds.[3] As a result, hair salons and some continually growing industries such as poultry farms, slaughterhouses, the wool industry and the tanning industry produce millions of tons of keratin-containing biomass. Because of no extensive quantity usage in any industry, human hair is considered a keratin-rich waste worldwide and its accumulation can cause many environmental problems. Also, there is no environmentally friendly disposal method for human hair, which is often landfilled or incinerated. Therefore, the conversion of human hair waste into a useful source for obtaining keratin will have significant implications for producing products for applications in the biomedical field, cosmetic products and environmental remediation.[4]

Human hair keratin mainly possesses α-helix structure (50–60%) and α-helices can form dimers linked by disulfide bonds.[5,6] In addition to the inter- and intramolecular disulfide bonds, hydrogen bonds, ionic bonds and hydrophobic interactions chemically

* *Correspondence to: Ö Erdemli, Department of Molecular Biology and Genetics, Başkent University, Ankara, 06790, Turkey, E-mail: oerdemli@baskent.edu.tr*

a *Department of Molecular Biology and Genetics, Başkent University, Ankara, Turkey*

b *Department of Biomaterials, University of Health Sciences Turkey, Istanbul, Turkey*

stabilize keratin and provide considerable mechanical properties.[4] Because of their ability to form biologically stable interactions and the lack of specific keratinases in mammals, keratins do not undergo rapid proteolytic degradation *in vivo* as is common with other biologically derived materials.[7] In addition to structural stability, human hair keratin contains cell adhesion motifs such as leucine–aspartic acid–valine (LDV) and arginine–glycine–aspartic acid (RGD).[8,9] Due to its excellent biocompatibility, unique chemical structure, biodegradability and capability to support cellular attachment, keratin has been recognized as an effective naturally derived biomaterial.[5,10] Keratin-based biomaterials for bone tissue regeneration have been reported in recent years. For example, human hair keratin/jellyfish collagen/eggshell-derived hydroxyapatite scaffolds fabricated by freeze-drying method enabled the self-differentiation of human adipose mesenchymal stem cells into osteogenic lineage without any induction agents.[11] Compared to collagen/hydroxyapatite scaffolds, keratin-containing scaffolds allowed the formation of a calcified matrix and significantly higher levels of osteopontin and osteonectin expressions by cells. Keratin has been shown to possess osteoinductive potential; in other words, it can stimulate the osteogenic differentiation of stem cells.[12] In another study, porous keratin–hydroxyapatite composite scaffolds were implanted in the long bones of adult sheep for up to 12 weeks to investigate the osteoconduction response compared to a collagen matrix.[13] Keratin–hydroxyapatite scaffolds showed a slower rate of degradation *in vivo* than collagen matrix and the rate of bone ingrowth into the keratin–hydroxyapatite scaffolds was consistent with the rate of keratin–hydroxyapatite resorption.

Despite the remarkable structural stability and biological properties of keratin, it needs to be mixed with other compounds to meet the strength and elastic modulus requirements of bone. To improve mechanical properties, combining keratin with hydrophobic polymers is an alternative way.

Polycaprolactone (PCL) is widely used in bone tissue engineering due to its superior mechanical properties, non-toxicity, tissue-compatible properties and longer degradation time (2–3 years).[14] However, PCL is unable to provide bioactivity such as osteoconductivity. To improve the mechanical properties, degradation rates and bioactivity of PCL, natural or synthetic polymers or inorganic fillers were added to PCL.[14] Different types of inorganic fillers such as hydroxyapatite,[15,16] tricalcium phosphate,[17] bioactive glass[18] and calcium carbonate ($CaCO_3$)[19] can be incorporated within PCL-based matrices to improve these properties for bone tissue engineering. Due to its close resemblance to the inorganic component of human bone, bioactivity and biocompatibility, hydroxyapatite has garnered significant interest in its incorporation into electrospun polymeric fibers. However, the morphology, crystallinity and degradation properties of synthesized hydroxyapatite are different from those of natural hydroxyapatite.[20,21] In some cases, the slow degradation of hydroxyapatite[22] can impede the natural healing process by inhibiting the timely replacement of the scaffold with newly formed bone.[23] As an alternative to hydroxyapatite, $CaCO_3$ offers better natural biodegradation properties and additionally it has outstanding properties that make it ideal for bone regeneration, including biocompatibility, bioactivity and high osteoconductivity.[24,25] In previous studies, $CaCO_3$ supported the osteogenesis of bone marrow mesenchymal stem cells more effectively than hydroxyapatite in the early stages.[26,27] In another study, the addition of $CaCO_3$ microspheres into fibrin-glue hydrogel improved the osteoconductivity.[28]

A common source of the production of $CaCO_3$ is the limestone magnesite from rocks. However, large-scale mining and production of limestone cause some environmental damage and high costs for environmental compliance.[29] Therefore, utilizing natural sources of $CaCO_3$ such as seashells and snail shells in the context of shell waste recovery can be environmentally friendly and economically feasible. Among the largest freshwater snails, the golden apple snail (*Pomacea canaliculata*) is a popular aquarium snail, and it can be also found in freshwater lakes, rivers, streams, ponds and marshes. This species is also a serious pest of paddy rice and aquatic plants.[30] Their shells are mainly composed of 99.3% $CaCO_3$, sodium oxide, silicon dioxide and other oxide types.[31] Calcium carbonate from snail shells as a biomaterial in bone tissue engineering helps make use of this readily available and sustainable resource, reducing the dependence on scarce or costly materials. Typically, $CaCO_3$ is encountered either in the amorphous calcium carbonate form or as one of the three polymorphs: calcite, vaterite or aragonite.[32] Among these calcium carbonate polymorphs, calcite is regarded as the most stable,[32] whereas vaterite is the least stable.[33,34] A previous study demonstrated that calcite nanoparticles supported osteogenesis in human mesenchymal stem cells.[35] Vaterite has the ability to transform into hydroxyapatite when exposed to simulated body fluid (SBF) or an organic fluid like interstitial body fluid.[33,34] Vaterite was shown to exhibit a pivotal role in promoting osteogenesis, supporting angiogenesis and facilitating the repair of bone defects in vaterite-coated PCL scaffolds during a 28-day implantation period in a rat femur defect.[36]

In the study reported here, electrospun PCL fibers incorporated with keratin and calcium carbonate were developed. In this regard, $CaCO_3$ was isolated from the shells of freshwater snails (*P. canaliculata*) and characterized using scanning electron microscopy (SEM) and Fourier transform infrared (FTIR) spectroscopy. Keratin was extracted from human hair waste by a reduction method and characterized using FTIR and sodium dodecyl sulfate polyacrylamide gel electrophoresis (SDS-PAGE). Two kinds of fibers were fabricated, namely PCL/keratin (PCL/Ker) and PCL/keratin/$CaCO_3$ (PCL/Ker/$CaCO_3$) fibers. These fibers were characterized using SEM, FTIR spectroscopy, differential scanning calorimetry (DSC) and thermogravimetric analysis (TGA). Additionally, *in vitro* bioactivity and *in vitro* cytotoxicity of the electrospun fibers were examined.

MATERIALS AND METHODS

Materials

PCL (Mw = 80 000 Da), 1,1,1,3,3,3-hexafluoro-2-propanol (HFIP), phosphate-buffered saline and all other reagents were purchased from Sigma-Aldrich, USA. Urea was supplied by Amresco Inc., UK. The 14 kDa dialysis membrane was from Bio Basic Inc., Canada. For SDS-PAGE analysis, BLUeye Prestained Protein Ladder and Coomassie Brilliant Blue R-250 were obtained from GeneDireX Inc., USA, and Serva Electrophoresis GmbH, Germany, respectively. GE Healthcare Whatman™ Qualitative Filter Paper Grade 1 was purchased from Fisher Scientific Pte. Ltd, Singapore.

Dulbecco's modified Eagle medium (DMEM), trypsin–EDTA (0.025%) and penicillin–streptomycin solution were purchased from Biowest, France. Fetal bovine serum (FBS) was supplied by Capricorn Scientific GmbH, Germany. Reagent alamarBlue™ was from Invitrogen, USA. All reagents were used as received.

Polymer International published by John Wiley & Sons Ltd on behalf of Society of Chemical Industry.

Isolation of calcium carbonate from freshwater snails

$CaCO_3$ was isolated from the shells of freshwater snails (*P. canaliculata*) (Fig. 1). Firstly, the shells were washed with distilled water and dried in an oven (Bicasa, Italy) for 24 h at 100 °C. After grinding with a mortar, the shell powder was mixed with 2.0 mol L^{-1} hydrochloric acid (HCl) in a 1:5 (w/v) ratio and stirred for 30 min using a magnetic stirrer (MSH-20A, Daihan Scientific, Korea) at room temperature. At the end of this reaction, the mixture was filtered through Whatman Grade No. 1 filter paper to remove impurities and large shell residues. Then, a 2.0 mol L^{-1} sodium carbonate (Na_2CO_3) solution, which had the same volume as the HCl solution, was added to the filtered solution to precipitate $CaCO_3$. $CaCO_3$ was separated by using filter paper and dried in an oven at 100 °C.

Isolation of keratin from human hair

Keratin was isolated from human hair samples collected from local barbershops (Fig. 2). Firstly, the hair samples were kept in a solution of chloroform–methanol (2:1, v/v) for 6 h to perform the delipidation process. After filtration through Whatman Grade No. 1 filter paper, delipidated hair samples were dried in an oven for 24 h at 70 °C. Dried hair samples were decolorized with the incubation in a solution of hydrogen peroxide–ammonia (2:1, v/v) for 15 min and subsequently they were dried in an oven for 4 h at 70 °C. Dried hair samples were added into the extraction solution prepared using 0.125 mol L^{-1} sodium sulfide (Na_2S), 0.500 mol L^{-1} sodium bisulfide ($NaHSO_3$), 8.00 mol L^{-1} urea and 0.100 mol L^{-1} SDS and stirred using a magnetic stirrer at 50 °C for 4 h. Then, the hair-extraction mixture was filtered and dialyzed against deionized water with a 12 kDa cellulose dialysis membrane for 5 days with changes at regular intervals at room temperature. After dialysis, obtained samples were lyophilized to obtain keratin in powder form.

Fabrication of electrospun PCL fibers containing keratin and calcium carbonate

To prepare the electrospun fibers, keratin isolated from human hair and PCL were separately dissolved in the solvent HFIP at a concentration of 10% (w/v). Afterward, PCL and keratin solutions were mixed at a ratio of 7:3 (v/v). The resulting solution was stirred overnight to obtain a homogeneous mixture, and then electrospinning was performed. To prepare calcium carbonate-containing fibers, calcium carbonate powder was added to the 10% PCL–HFIP solution at a ratio of 1:10 (w/v) before mixing with the keratin solution. Electrospinning was performed with an electrospinning setup (Fytronix, Turkey). Each prepared solution was dispensed from a single nozzle (22 gauge) at a constant flow rate of 1 mL h^{-1} and electrospun at 20 kV. PCL, PCL/Ker and PCL/Ker/$CaCO_3$ fibers were collected on a grounded, flat metallic platform fixed at 14 cm below the tip of the nozzle.

Morphological, physicochemical and thermal characterizations

The microstructural properties of $CaCO_3$ and fabricated fibers were investigated using SEM (JEOL NeoScope JCM-7000, Japan) without any conductive coating at an accelerating voltage of 15 and 5 kV, respectively. The particle size analysis of $CaCO_3$ particles was performed on SEM images utilizing FIJI (ImageJ, NIH, USA) software. A randomized approach was employed to measure the sizes of 100 individual particles from the SEM images. Likewise, the mean diameters of fibers were ascertained by measuring randomly selected fiber diameters extracted from the SEM images ($n = 100$).

The crystalline structure of isolated $CaCO_3$ was evaluated using a powder X-ray diffraction (XRD) system (Empyrean, Malvern Panalytical, Malvern, UK), equipped with a Cu Kα1 radiation source. The diffraction angle (2θ) was varied from 20° to 80° using a scanning speed of 2° min^{-1}.

The chemical properties of $CaCO_3$, lyophilized keratin, PCL fibers, PCL/Ker fibers and PCL/Ker/$CaCO_3$ fibers were investigated by attenuated total reflectance (ATR) FTIR spectroscopy (Nicolet iS50, ThermoFisher, France). The samples were positioned on the ATR crystal plate and subjected to scanning at room temperature, covering a spectral range from 500 to 4000 cm^{-1} in absorbance mode, with a resolution of 4 cm^{-1}.

Additionally, lyophilized keratin was examined using SDS-PAGE. An acrylamide/bisacrylamide separating gel with 1.5 mol L^{-1} Tris–HCl buffer at pH 8.8 and a stacking gel with 0.5 mol L^{-1} Tris–HCl buffer at pH 6.8 were used. Firstly, keratin solutions were incubated for 2 min at 95 °C in Laemmli sample buffer before

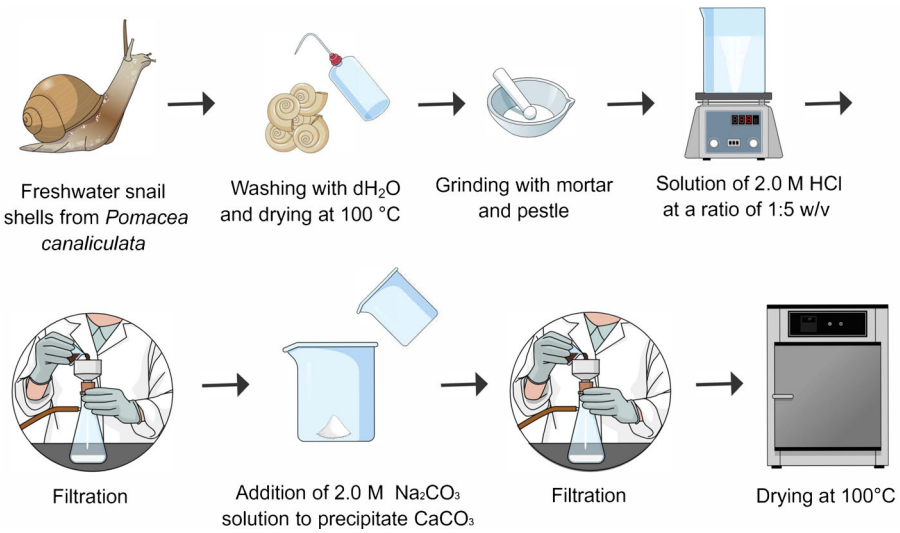

Figure 1. Schematic depicting the process for isolating calcium carbonate from freshwater snail shells.

Polymer International published by John Wiley & Sons Ltd on behalf of Society of Chemical Industry.

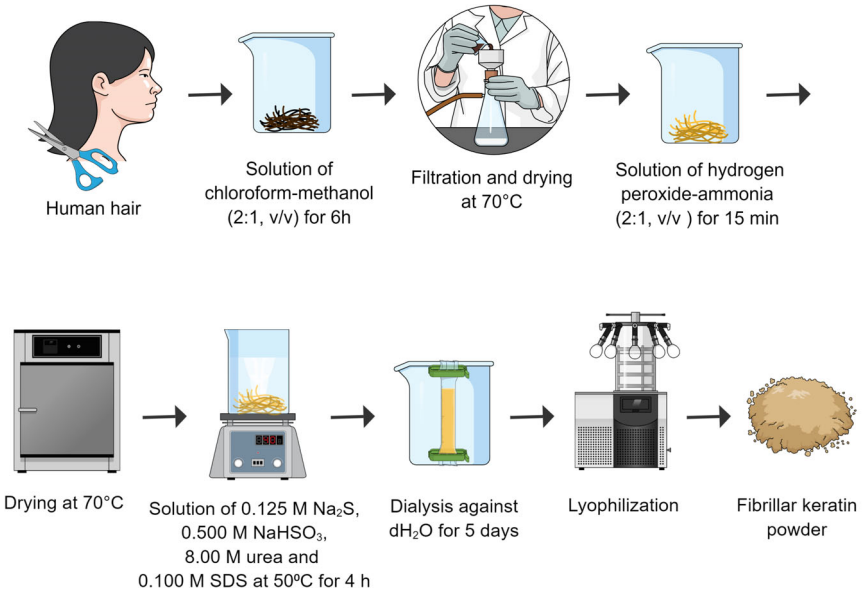

Figure 2. Schematic detailing the method for isolating keratin from human hair.

loading on the gel. Afterward, keratin solution and Protein Ladder were loaded into the gel wells. The electrophoresis was run at 100 V for 1 h by using a vertical electrophoresis system (Hoefer Scientific Instruments, San Francisco, CA). After electrophoresis, the gels were washed with deionized water and stained with Coomassie Brilliant Blue R-250.

The thermal properties of the fibers were analyzed using DSC (DSC8000, PerkinElmer, USA). The samples underwent a temperature program involving two heating cycles, ranging from −70 to 230 °C, with a heating rate of 10 °C min^{-1}, all under a nitrogen atmosphere.

TGA curves of PCL, PCL/Ker and PCL/Ker/$CaCO_3$ fibers were generated using a TGA device (TGA8000, PerkinElmer, USA) under a nitrogen atmosphere with a gas flow rate of 20 mL min^{-1}. The samples underwent heating from 25 to 600 °C at a ramp rate of 10 °C min^{-1}. The analysis software provided by the equipment was utilized to determine the remaining weight percentages.

In vitro bioactivity

To determine the *in vitro* bioactivity of the PCL, PCL/Ker and PCL/Ker/$CaCO_3$ fibers, the electrospun fibers were soaked in 5 mL of SBF (pH 7.4) at 37 °C for 7 days. SBF was prepared by a method described in the literature.[37] At the end of the 7th day, soaked fibers were taken out and rinsed three times with deionized water. Finally, they were dried at 40 °C overnight and characterized by SEM.

In vitro cell viability

The human osteogenic sarcoma cell line (Saos-2) was used for *in vitro* cell viability studies. Cells were cultured in DMEM–high glucose with stable glutamine containing 10% (v/v) FBS and 100 U mL^{-1} streptomycin/penicillin at 37 °C under a humidified atmosphere of 5% CO_2 in an incubator (PHCbi Corp., Japan). The medium was changed after every 3 days. Cells were detached with trypsin (0.25%)–EDTA (0.02%) in Hank's balanced salt solution for passaging.

Electrospun fibers were sterilized by UV exposure for 30 min on each side of the sample. An amount of 100 µL of Saos-2 cell suspension with a density of 3.6×10^4 cells mL^{-1} was seeded on the sterilized PCL, PCL/Ker and PCL/Ker/$CaCO_3$ fibers as well as with no material (cells seeded on tissue culture plate (TCP) was considered as control group) and incubated in a CO_2 incubator at 37 °C for 1, 2, 3, 7 and 14 days ($n = 5$). To study cell viability on fibers, an Alamar Blue assay was performed. After each incubation period, cell culture media were removed, and fiber and control groups were rinsed with phosphate-buffered saline (pH 7.20). Then, phosphate-buffered saline was replaced with DMEM containing 10% (v/v) Alamar Blue, and the samples were incubated at 37 °C for 3 h in a CO_2 incubator. After incubation, the Alamar Blue solution of groups was transferred into a 96-well plate and the absorbances were recorded at 570 and 600 nm utilizing a microplate reader (Epoch BioTek, USA). The same procedure was also applied to fiber groups without cell seeding to include Alamar Blue percent reduction calculations.

Statistical analysis

All data are expressed as mean ± standard deviation. Statistical differences were determined by one-way analysis of variance followed by *post hoc* Tukey test by utilizing the SPSS Version 26.0 and differences were considered statistically significant at $P \leq 0.05$.

RESULTS

Morphological, physicochemical and thermal characterizations

For the preparation of PCL/Ker/$CaCO_3$ fibers, $CaCO_3$ was isolated from the shells of freshwater snails (*P. canaliculata*). The isolated $CaCO_3$ has been found to exhibit two polymorphs, namely vaterite and calcite, as revealed by SEM, XRD and FTIR analysis.

SEM images of $CaCO_3$ used in the fabrication of fibers are given in Fig. 3(a),(b). $CaCO_3$ isolated from *P. canaliculata* shells was observed to be composed of mostly spherical and some minor amount of rod-like particles. The mean size of $CaCO_3$ particles is found to be 3.56 ± 1.66 µm.

Polymer International published by John Wiley & Sons Ltd on behalf of Society of Chemical Industry.

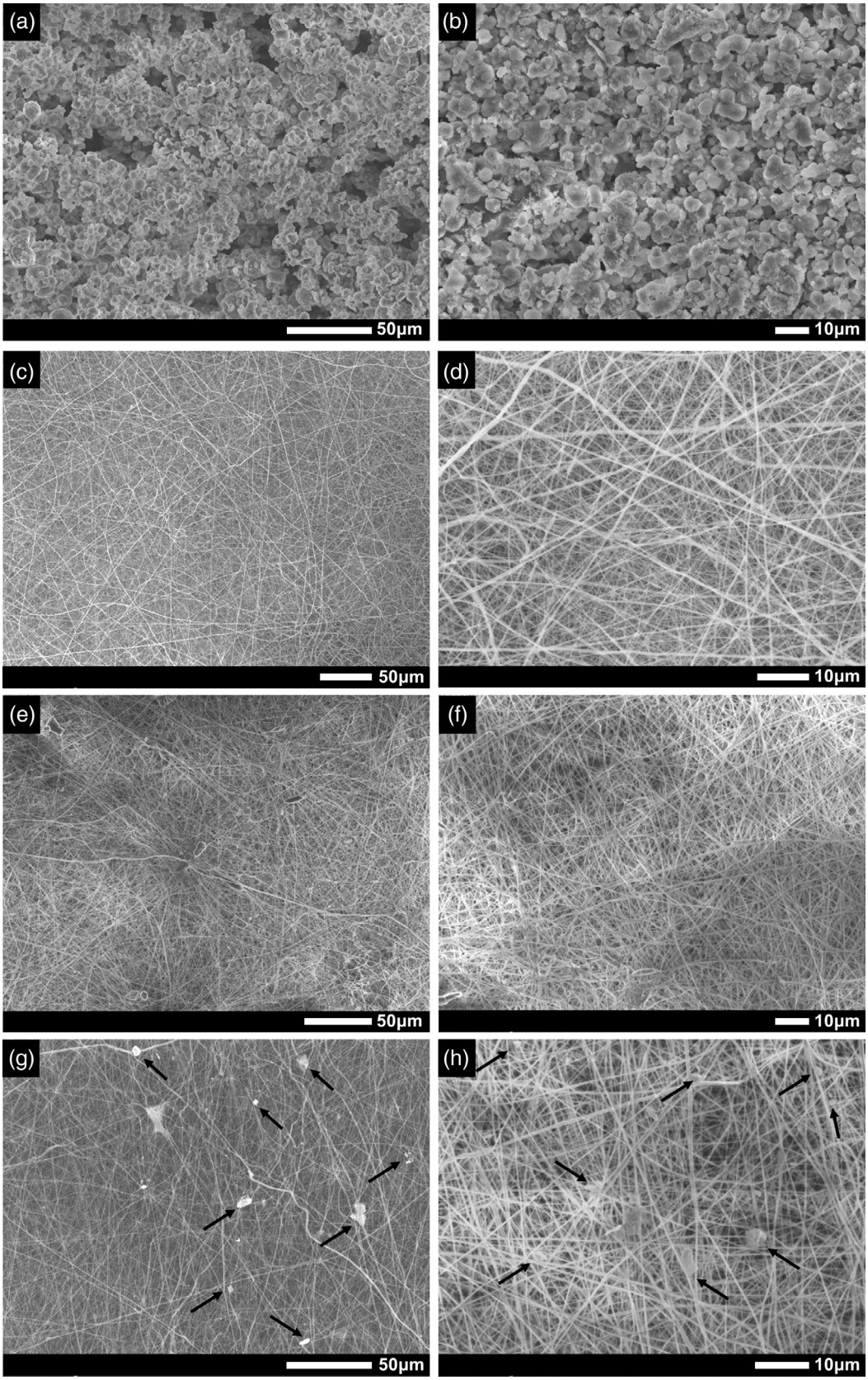

Figure 3. SEM images of $CaCO_3$ (a, b); PCL fibers (c, d); PCL/Ker fibers (e, f); and PCL/Ker/$CaCO_3$ fibers (g, h). Arrows indicate selected $CaCO_3$ depositions on fibers.

Polymer International published by John Wiley & Sons Ltd on behalf of Society of Chemical Industry.

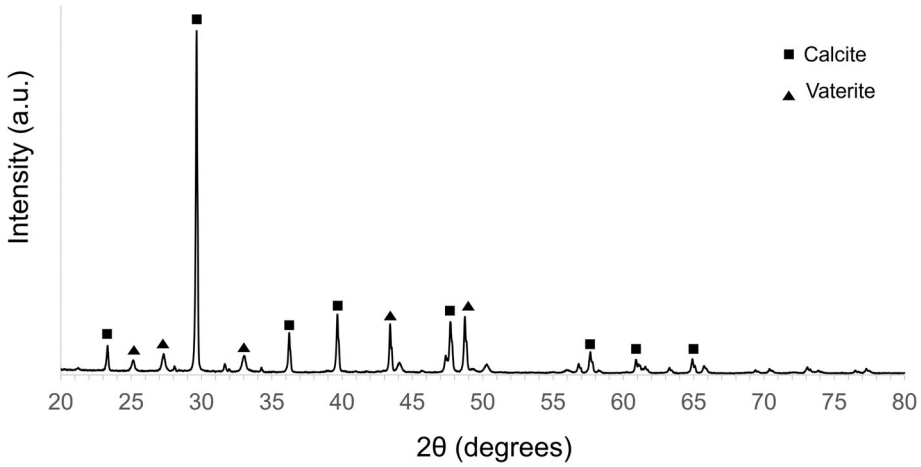

Figure 4. Powder XRD pattern of isolated $CaCO_3$ (calcite and vaterite phases are denoted by squares and triangles, respectively).

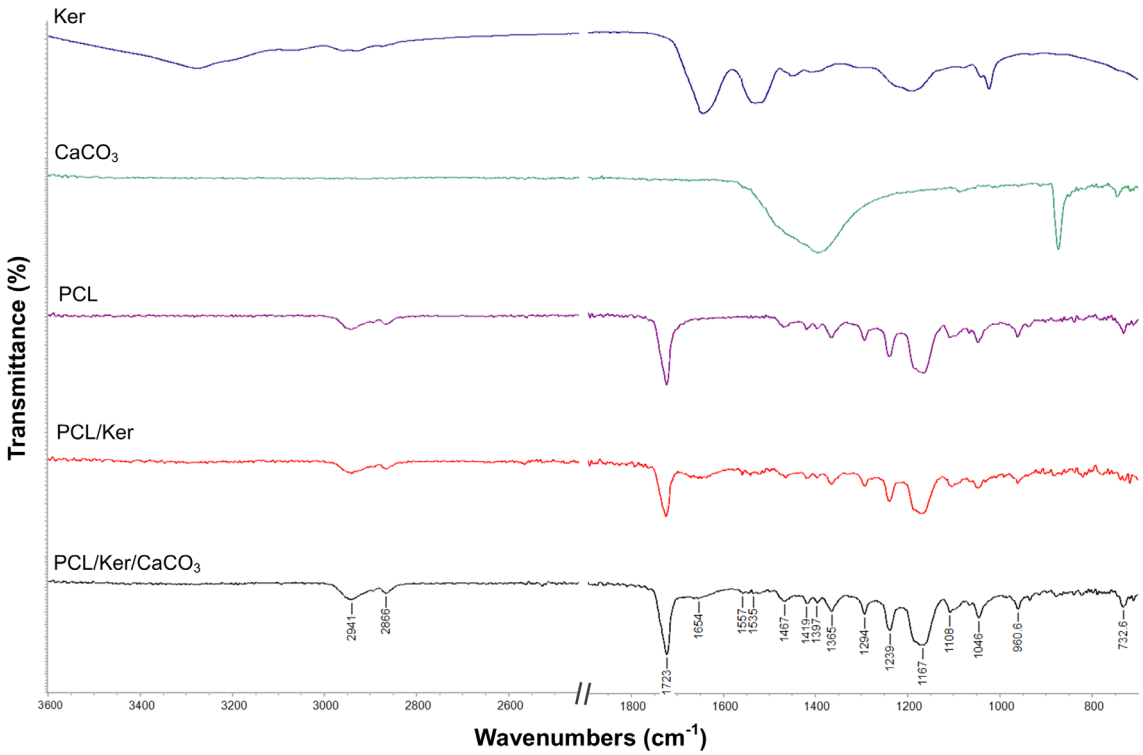

Figure 5. FTIR spectra of $CaCO_3$, keratin (Ker), PCL, PCL/Ker fibers and PCL/Ker/$CaCO_3$ fibers.

SEM images of PCL, PCL/Ker and PCL/Ker/$CaCO_3$ fibers at different magnifications are given in Fig. 3(c)–(h). As seen in Fig. 3(c),(d), random PCL fibers were produced, and a notable observation was the absence of bead formation along the fiber structures. The mean diameter of PCL fibers was measured at 457 ± 345 nm (Fig. 1(d)). On the other hand, the SEM images in Fig. 3(e),(f) reveal the presence of a limited number of clusters on the random PCL/Ker fibers. The average diameter of the PCL/Ker fibers, measured from Fig. 3(f), was determined to be 371 ± 103 nm. Moreover, PCL/Ker/$CaCO_3$ fibers have some clusters and $CaCO_3$ particles (Fig. 3(g),(h)). The mean diameter of PCL/Ker/$CaCO_3$ fibers was found to be 258 ± 76 nm from Fig. 3(h).

The XRD pattern of isolated $CaCO_3$ is given in Fig. 4. The peaks are indexed to vaterite (ICDD: 00-033-0268) or calcite (ICDD: 00-005-0586) polymorphs.[38] The characteristic peaks of vaterite at 25.15°, 27.29° and 33.01°, and those of calcite at 29.65°, 36.22° and 39.66° were recorded, aligning with the literature.[39]

FTIR spectra of $CaCO_3$ isolated from the shells of *P. canaliculata*, keratin isolated from human hair, PCL fibers, PCL/Ker fibers and PCL/Ker/$CaCO_3$ fibers are given in Fig. 5. In the FTIR spectrum of $CaCO_3$, the absorption band at around 1395 cm^{-1} can be assigned to the stretching vibration of the C═O bond in the carboxylate of $CaCO_3$. Additionally, the absorption bands of carbonate at 1395 (asymmetric stretching, ν_3 mode), 1088 (symmetric

Polymer International published by John Wiley & Sons Ltd on behalf of Society of Chemical Industry.

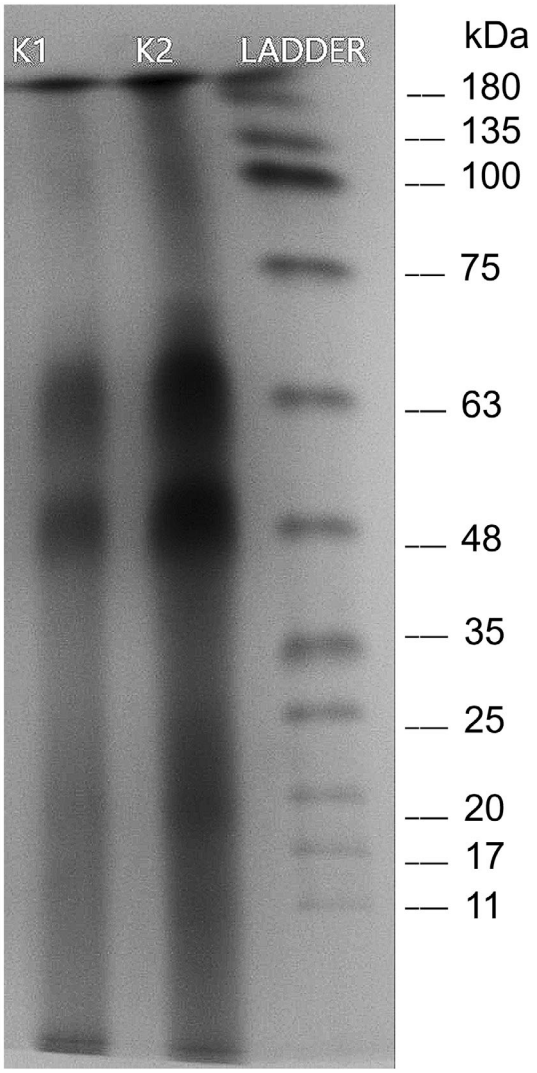

Figure 6. SDS-PAGE analysis of keratin isolated from human hair. Lane 1 (K1) and 2 (K2): two different Coomassie Blue-stained samples of isolated keratin. Lane 3: protein ladder.

stretching, ν_1 mode), 873 (out-of-plane bending, ν_2 mode) and 746 cm^{-1} (in-plane bending, ν_2 mode) could be attributed to the characteristic vaterite bands.[40,41] The bands of carbonate out-of-plane bending (ν_2 mode) and in-plane bending (ν_4 mode) vibrations of calcite are expected to appear at 876 and 713 cm^{-1}.[40] For the FTIR spectrum of keratin, the absorption peaks at 1644 and 1531 cm^{-1} ae attributed to the C═O stretching vibration of the amide I structure[8] and the N—H bending and C—H stretching vibration peak of the amide II structure,[42] respectively. The broad absorption band at about 1197 cm^{-1} is attributed to the C—N stretching and C═O bending vibrations of amide III.[43] The absorption band at 3295 cm^{-1} can be assigned to peptide bonds (—CONH–) known as amide A.[42] In addition, the absorption peak at 1024 cm^{-1} could be attributed to the S—O symmetric stretching vibration of cysteine-S sulfonate residue.[8] The FTIR spectrum of PCL shows asymmetric and symmetric CH_2 stretching peaks at 2941 and 2867 cm^{-1}, respectively.[44] The characteristic carbonyl (C═O) stretching has a strong absorption band at 1723 cm^{-1}.[44] The remaining absorption bands can be assigned to CH_2 bending (1469, 1419 and 1365 cm^{-1}), C—O—C stretching (1239, 1109 and 1048 cm^{-1}), C—O stretching (1165 cm^{-1}) and C—C stretching (1294 cm^{-1}).[44] The spectra of PCL/Ker fibers and PCL/Ker/$CaCO_3$ fibers showed the characteristic absorption bands of PCL, keratin and $CaCO_3$ but the relative strengths and positions of these bands changed.

Structural stability and the molecular masses of the isolated keratin proteins were investigated by the SDS-PAGE method (Fig. 6). Isolated keratin has α-keratin (45 kDa) and β-keratin (63 kDa) structures.

In Fig. 7, the DSC curves obtained from the second heating scan of PCL, PCL/Ker and PCL/Ker/$CaCO_3$ fibers are presented. The peak temperatures (T_m) on the graph indicate the average melting temperature of the crystallites, measured as 74.41, 77.09 and 76.17 °C for PCL, PCL/Ker and PCL/Ker/$CaCO_3$ fibers, respectively. Additionally, the onset temperatures (T_{on}) were determined to be 69.30, 74.37 and 72.88 °C, respectively, for the same samples.

Figure 8 displays the TGA curves of PCL, PCL/Ker and PCL/Ker/$CaCO_3$ fibers, wherein the remaining material weight percentages are 0.42%, 7.49% and 9.59%, respectively. The TGA curves exhibit distinct thermal degradation patterns. Specifically, PCL fibers exhibit a single-stage thermal degradation profile, while keratin-containing fibers show one major step and two smaller steps of mass loss.

In vitro bioactivity

PCL, PCL/Ker and PCL/Ker/$CaCO_3$ fibers were fabricated using electrospinning and subsequently immersed in SBF for 7 days to assess their *in vitro* bioactivity as fibers. After 7 days, the morphological characteristics of the tissue fibers maintained in SBF were analyzed using SEM (Fig. 9). Remarkably, the SEM images demonstrated the nucleation of apatite on the surface of all fibers exposed to SBF.

In vitro cell viability

The cell viability on the PCL, PCL/Ker and PCL/Ker/$CaCO_3$ fibers was assessed using the Alamar Blue assay. Figure 10 shows the Saos-2 cell viability on fibers after 1, 2, 3, 7 and 14 days of cell culture with respect to control (TCP). No significant differences were observed among any of the groups compared to the control after the second day of incubation. The increase in cell viability observed on the first day is due to the larger surface area of the fiber structures compared to TCP, resulting in enhanced cellular attachment.

DISCUSSION

The development of sustainable biomaterials for tissue engineering holds crucial importance in addressing the ever-growing demand for effective solutions in regenerative medicine. In this context, the utilization of electrospun PCL scaffolds enriched with freshwater snail calcium carbonate and waste human hair keratin is explored as a sustainable approach for bone tissue engineering. For the preparation of PCL/Ker/$CaCO_3$ fibers, $CaCO_3$ was isolated from the shells of freshwater snails (*P. canaliculata*). The isolated $CaCO_3$ was found to exhibit two polymorphs, namely vaterite and calcite, as revealed by XRD, FTIR and SEM analysis. The XRD pattern of $CaCO_3$ exhibited remarkably sharp peaks, which were obtained without the need for heat treatment, in contrast to previous studies.[29,45] This finding underscores the efficiency of the isolation method in obtaining highly crystalline $CaCO_3$ without the necessity of calcination. Similarly, the successful isolation of keratin from human hair was confirmed through

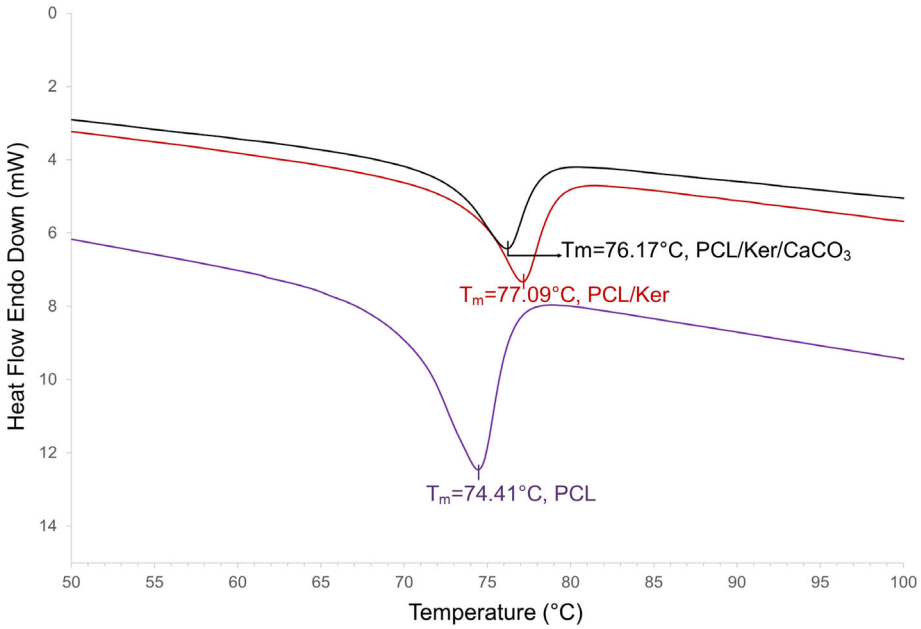

Figure 7. DSC curves during the second heating scan of PCL, PCL/Ker and PCL/Ker/$CaCO_3$ fibers. The plot displays peak temperatures (T_m) representing the average melting temperature of the crystallites, labeled accordingly.

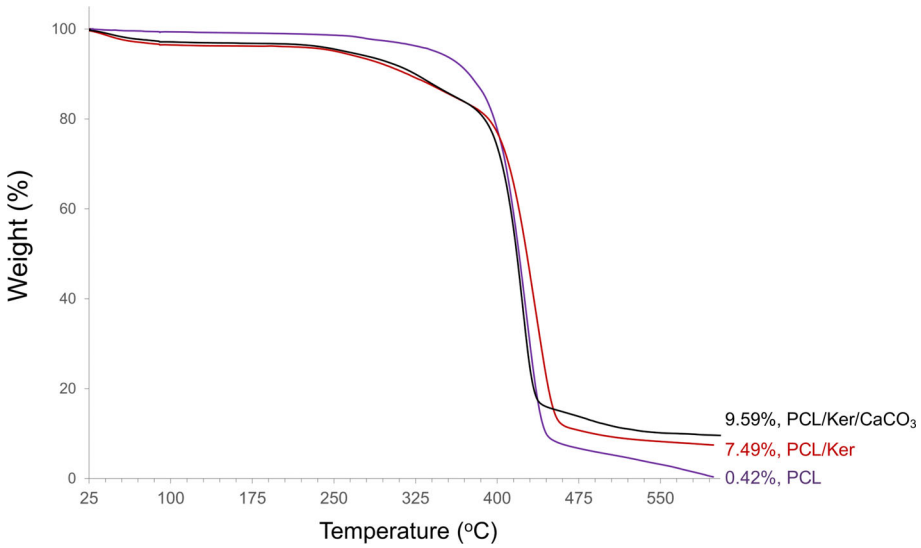

Figure 8. TGA curves of PCL, PCL/Ker and PCL/Ker/$CaCO_3$ fibers.

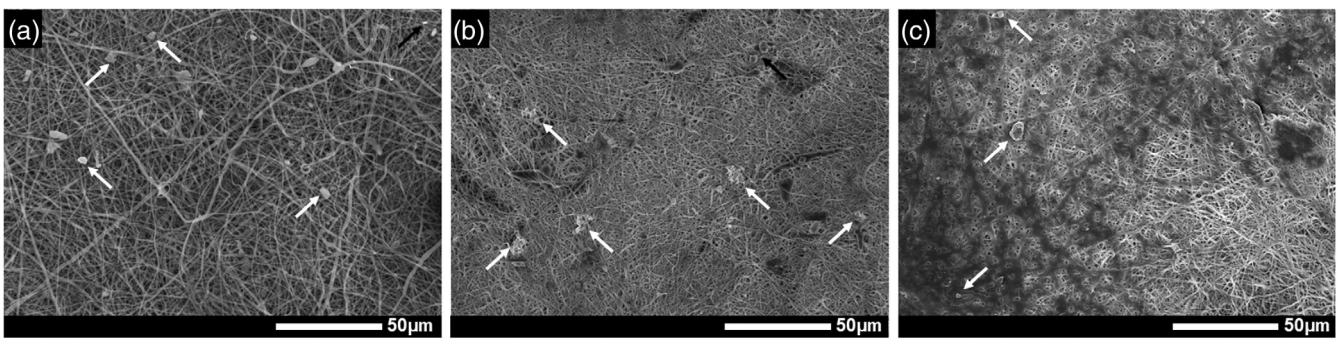

Figure 9. SEM images of PCL, PCL/Ker and PCL/Ker/$CaCO_3$ fibers kept in SBF for 7 days. Arrows indicate selected inorganic depositions on fibers.

Polymer International published by John Wiley & Sons Ltd on behalf of Society of Chemical Industry.

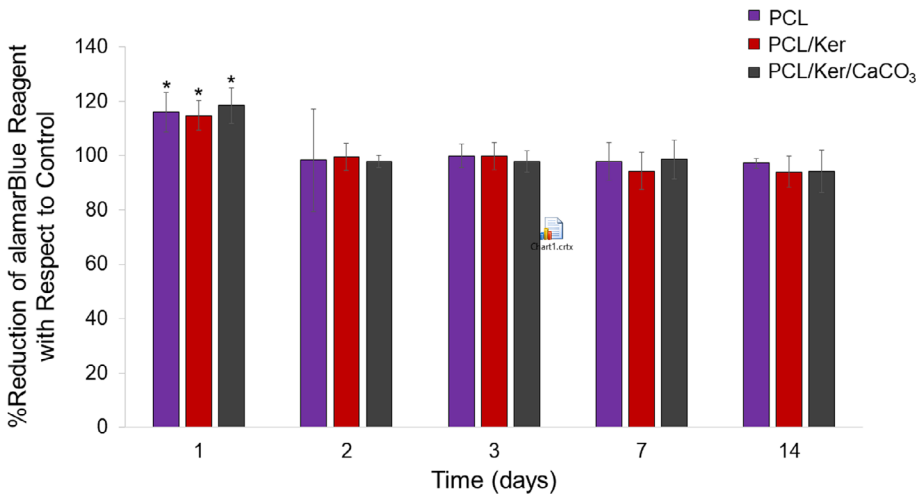

Figure 10. Saos-2 cell viability on PCL, PCL/Ker and PCL/Ker/$CaCO_3$ fibers (percent reduction of alamarBlue reagent with respect to control (TCP)) (*$P < 0.05$).

SDS-PAGE and FTIR analysis, revealing the presence of α-keratin structures of around 45–50 kDa and β-keratin structures of around 55–60 kDa, as demonstrated in a previous study.[11]

According to SEM studies, it was observed that the diameter of PCL/Ker fibers was thinner than that of pure PCL fibers, and this diameter was further reduced with the addition of $CaCO_3$. These observations align with findings from a previous study,[46] which reported that the incorporation of keratin into PCL led to a significant decrease in fiber diameter from 552 ± 66 to 196 ± 51 nm. This reduction in fiber diameter was attributed to the increased electroconductivity of the electrospinning solution with the addition of keratin. The amino acid groups of keratin conferred negative charges to the protein, thereby enhancing the solution's electroconductivity. Such nano-sized fibers have been reported to be beneficial for improving cell adhesion and proliferation. Furthermore, it was also confirmed in another study[47] that the presence of keratin resulted in narrower diameter distributions, whereas PCL/gelatin fibers exhibited wider diameter distributions, potentially as a result of difficulties in achieving homogeneous gelatin mixing in the HFIP solution.

On the other hand, while SEM studies demonstrate a reduction in fiber diameter with the addition of $CaCO_3$ to the PCL/Ker matrix, contrasting findings have been reported in previous studies. According to the findings of an earlier study,[48] which investigated the incorporation of ellipsoidal $CaCO_3$ into a chitosan/poly(vinyl alcohol) (PVA) mixture followed by electrospinning, it was observed that the addition of $CaCO_3$ resulted in the formation of web-like nanofiber connections among electrospun chitosan/PVA fibers. The diameters of fibers increased from 71.5 ± 23.4 to 281.9 ± 51.2 nm for 9 wt% of $CaCO_3$ loading. The branch fibers were attributed to the instability of the polymer jet induced by the presence of ellipsoidal calcium carbonate. Unlike chitosan/PVA, PCL/Ker did not show instability in the present study. This highlights the complexity of interactions between different polymer systems and $CaCO_3$.

According to the results of DSC analysis, the incorporation of keratin into PCL results in a slight upward shift in the melting onset and peak temperatures, while the addition of $CaCO_3$ leads to a 1 °C decrease in these values. A previous study indicated that the inclusion of 10% wool had a negligible impact on the melting point of PCL,[48] which is consistently reported to be around 71 °C,[49,50] aligning with the results of this study. Based on the TGA curves, it can be observed that the mass loss of the keratin-containing (PCL/Ker and PCL/Ker/$CaCO_3$) fibers started at lower temperatures in comparison to the pure PCL group. This difference in mass loss can be attributed to the release of sulfur dioxide and hydrogen sulfide reported in the literature, which typically occurs between 230 and 250 °C due to the breakage of disulfide bonds.[51] The residual ash contents in the TGA thermograms can be attributed to the residual quantities of keratin and $CaCO_3$ within the PCL matrix, considering that pure PCL was almost entirely consumed. Specifically, for the PCL/Ker/$CaCO_3$ fibers initially containing 10% (w/w) $CaCO_3$, a remaining ash content of 9.59% was observed.

The assessment of bioactivity in SBF revealed the presence of a minimal quantity of mineral deposits on the pure PCL scaffold, aligning with earlier findings in the literature concerning electrospun PCL scaffolds.[52] As previously explained, hydrolytic degradation of PCL primarily involves the cleavage of ester bonds on the surface of PCL fibers, resulting in the formation of carboxyl (–COOH) and hydroxyl (–OH) groups. This process is followed by the electrostatic attraction between Ca^{2+} cations and the negatively charged groups on the fiber surface, resulting in the formation of hydroxyapatite crystals containing PO_4^{3-} ions. Similarly, the presence of calcium phosphate accumulation has been noted on the PCL/Ker and PCL/Ker/$CaCO_3$ fibers. However, this accumulation did not advance beyond the nucleation stage, since the restricted 7-day timeframe within the SBF was inadequate to facilitate substantial mineral deposition. It is known that the growth of the apatite layer in SBF depends on factors such as surface area, incubation time, solution temperature and ionic concentration. The process of calcium phosphate accumulation may extend for a duration of 4 to 8 weeks, even with 10% hydroxyapatite in electrospun PCL-based fibers acting as nucleation sites,[53] or with 30% calcium silicate and bioactive glass (BG45S5) by weight.[54] As a result, increasing the amount of $CaCO_3$ was considered to help facilitate the nucleation and acceleration of mineralization.

As indicated by the outcomes of the Alamar Blue assay, it was determined that PCL, PCL/Ker and PCL/Ker/$CaCO_3$ fibers are non-toxic and offer sufficient support for the growth and proliferation of Saos-2 cells. Likewise, it was reported that there was no significant difference in the proliferation of fibroblast cells (3T3)

between PCL/keratin fibers (70:30) and TCP.[55] In contrast, PCL/keratin fibers (50:50) exhibited an enhancement in the viability of human mesenchymal stem cells compared to pure electrospun PCL fibers.[47] This increase in human mesenchymal stem cell proliferation was attributed to the presence of RGD-like and LDV-like adhesion motifs within the keratin structure, which improved the interaction between cells and the materials. Given the limited influence of $CaCO_3$ addition on Saos-2 cell proliferation observed in this study, it is apparent that further optimization is necessary for the successful addition of $CaCO_3$ and keratin into PCL fibers. Future studies should comprehensively investigate their potential effects on the adhesion, proliferation and differentiation of bone cells, taking into account a broader array of material proportions to gain a more comprehensive understanding of their biological consequences.

CONCLUSION

This study presents a novel approach to sustainable biomaterials for tissue engineering by harnessing the synergistic potential of freshwater snail-derived calcium carbonate and waste human hair-derived keratin to enhance electrospun PCL scaffolds. The main conclusions of this study are the following.

- Keratin was effectively extracted from human hair, and $CaCO_3$ in the form of vaterite and calcite was obtained from freshwater snail shells.
- PCL/Ker and PCL/Ker/$CaCO_3$ fibers were fabricated via an electrospinning process, utilizing a weight ratio of 70:30 for PCL to keratin, with the addition of 10% $CaCO_3$ nanoparticles by weight to the PCL/Ker solution.
- The morphology analysis of electrospun fibers, PCL, PCL/Ker and PCL/Ker/$CaCO_3$, revealed a smooth nanostructure without any observable bead formations.
- The addition of keratin and $CaCO_3$ did not have a substantial impact on the melting point of the PCL fibers. However, thermal degradation was observed to initiate at lower temperatures in the PCL/Ker and PCL/Ker/$CaCO_3$ fibers, attributed to the decomposition process of keratin within these composite materials.
- While calcium phosphate accumulation was observed on the PCL/Ker and PCL/Ker/$CaCO_3$ fibers, it did not progress beyond the nucleation stage within the limited 7-day timeframe in SBF. This suggests that further optimization is required to facilitate substantial mineral deposition.
- The PCL, PCL/Ker and PCL/Ker/$CaCO_3$ fibers exhibited nontoxicity and supported the growth and proliferation of Saos-2 cells.

Overall, this study not only underscores the potential of PCL-based fibers incorporated with keratin and $CaCO_3$ for bone tissue engineering applications, but also highlights the importance of further exploration and optimization in this promising field.

ACKNOWLEDGEMENTS

The study was partially supported by the Scientific and Technological Research Council of Türkiye (TÜBİTAK) under the Research Project Support Programme for Undergraduate Students (2209-A). The FTIR, SEM, DSC and TGA experiments were performed at the Experimental Medicine Research and Application Center, University of Health Sciences Turkey.

CONFLICT OF INTEREST STATEMENT

The authors state that there are no conflicts of interest to disclose.

AUTHOR CONTRIBUTIONS

ÖE contributed toward conceptualization, methodology, supervising keratin and $CaCO_3$ isolation and characterization and *in vitro* cell viability analysis, writing and original manuscript preparation. BY contributed toward conceptualization, methodology, supervising fabrication and characterization of electrospun fibers, visualization, writing, reviewing and editing of the manuscript. İGS contributed to keratin and $CaCO_3$ isolation and fabrication of electrospun fibers and acquisition of data. ES helped in the fabrication and characterization of electrospun fibers and the acquisition of data.

REFERENCES

1 Joyce K, Fabra GT, Bozkurt Y and Pandit A, *Signal Transduct Target Ther* **6**:122 (2021). https://doi.org/10.1038/s41392-021-00512-8.
2 Brovold M, Almeida JI, Pla-Palacín I, Sainz-Arnal P, Sánchez-Romero N, Rivas JJ *et al.*, *Adv Exp Med Biol* **1077**:421–449 (2018). https://doi.org/10.1007/978-981-13-0947-2_23.
3 Donato RK and Mija A, *Polymers* **12**:32 (2019). https://doi.org/10.3390/polym12010032.
4 Senthilkumar N, Chowdhury S and Sanpui P, *J Mater Cycles Waste Manage* **25**:1–16 (2023). https://doi.org/10.1007/s10163-022-01492-9.
5 Rajabi M, Ali A, McConnell M and Cabral J, *Mater Sci Eng C* **110**:110612 (2020). https://doi.org/10.1016/j.msec.2019.110612.
6 Lee H, Noh K, Lee SC, Kwon I-K, Han D-W, Lee I-S *et al.*, *Tissue Eng Regener Med* **11**:255–265 (2014). https://doi.org/10.1007/s13770-014-0029-4.
7 Burnett LR, Rahmany MB, Richter JR, Aboushwareb TA, Eberli D, Ward CL *et al.*, *Biomaterials* **34**:2632–2640 (2013). https://doi.org/10.1016/j.biomaterials.2012.12.022.
8 Mohamed JMM, Alqahtani A, Fatease AA, Alqahtani T, Khan BA, Ashmitha B *et al.*, *Pharmaceuticals* **14**:781 (2021). https://doi.org/10.3390/ph14080781.
9 Verma V, Verma P, Ray P and Ray AR, *Biomed Mater* **3**:025007 (2008). https://doi.org/10.1088/1748-6041/3/2/025007.
10 Feroz S, Muhammad N, Ratnayake J and Dias G, *Bioact Mater* **5**:496–509 (2020). https://doi.org/10.1016/j.bioactmat.2020.04.007.
11 Arslan YE, Arslan TS, Derkus B, Emregul E and Emregul KC, *Colloids Surf B* **154**:160–170 (2017). https://doi.org/10.1016/j.colsurfb.2017.03.034.
12 Wu Y-L, Lin C-W, Cheng N-C, Yang K-C and Yu J, *J Biomed Mater Res B* **105**:180–192 (2017). https://doi.org/10.1002/jbm.b.33551.
13 Dias GJ, Mahoney P, Hung NA, Sharma LA, Kalita P, Smith RA *et al.*, *J Biomed Mater Res B* **105**:2034–2044 (2017). https://doi.org/10.1002/jbm.b.33735.
14 Dwivedi R, Kumar S, Pandey R, Mahajan A, Nandana D, Katti DS *et al.*, *J Oral Biol Craniofac Res* **10**:381–388 (2020). https://doi.org/10.1016/j.jobcr.2019.10.003.
15 Linh NVV, Du NT, My NTN, Tuyen NN, Phu HD and Tram NXT, *Mater Today: Proc* **66**:2895–2899 (2022). https://doi.org/10.1016/j.matpr.2022.06.553.
16 Sultana N and Hayat Khan T, *J Bionanosci* **7**:169–173 (2013). https://doi.org/10.1166/jbns.2013.1112.
17 Alehosseini M, Golafshan N and Kharaziha M, *Mater Today: Proc* **5**:15783–15789 (2018). https://doi.org/10.1016/j.matpr.2018.04.192.
18 Tabia Z, Akhtach S, Bricha M and El Mabrouk K, *Eur Polym J* **161**:110841 (2021). https://doi.org/10.1016/j.eurpolymj.2021.110841.
19 Cao Z, Wang D, Lyu L, Gong Y and Li Y, *RSC Adv* **6**:10641–10649 (2016). https://doi.org/10.1039/C5RA22548E.
20 Turnbull G, Clarke J, Picard F, Riches P, Jia L, Han F *et al.*, *Bioact Mater* **3**:278–314 (2018). https://doi.org/10.1016/j.bioactmat.2017.10.001.
21 Palmer LC, Newcomb CJ, Kaltz SR, Spoerke ED and Stupp SI, *Chem Rev* **108**:4754–4783 (2008). https://doi.org/10.1021/cr8004422.
22 Zhang Q, Wang W, Schmelzer E, Gerlach J, Liu C and Nettleship I, *J Biomed Mater Res A* **109**:859–868 (2021). https://doi.org/10.1002/jbm.a.37077.

23 Godavitarne C, Robertson A, Peters J and Rogers B, *Dent Traumatol* **31**: 316–320 (2017). https://doi.org/10.1016/j.mporth.2017.07.011.
24 Woldetsadik AD, Sharma SK, Khapli S, Jagannathan R and Magzoub M, *ACS Biomater Sci Eng* **3**:2457–2469 (2017). https://doi.org/10.1021/acsbiomaterials.7b00301.
25 Tollemar V, Collier ZJ, Mohammed MK, Lee MJ, Ameer GA and Reid RR, *Genes Dis* **3**:56–71 (2016). https://doi.org/10.1016/j.gendis.2015.09.004.
26 Suzawa Y, Kubo N, Iwai S, Yura Y, Ohgushi H and Akashi M, *Int J Mol Sci* **16**:14245–14258 (2015). https://doi.org/10.3390/ijms160614245.
27 Liu X and Wang Z, *Smart Mater Med* **4**:552–561 (2023). https://doi.org/10.1016/j.smaim.2023.04.004.
28 Gong Y, Zhang Y, Cao Z, Ye F, Lin Z and Li Y, *Biomater Sci* **7**:3614–3626 (2019). https://doi.org/10.1039/c9bm00463g.
29 Laonapakul T, Ratchawoot S, Patamaporn C, Yoshiharu M and Prinya C, *ScienceAsia* **45**:10–20 (2019). https://doi.org/10.2306/scienceasia1513-1874.2019.45.010.
30 Laonapakul T, Sutthi R, Chaikool P, Talangkun S, Boonma A and Chindaprasirt P, *Mater Sci Eng C* **118**:111333 (2021). https://doi.org/10.1016/j.msec.2020.111333.
31 Tepsila S and Suksri A, *IOP Conf Ser Earth Environ Sci* **113**:012206 (2018). https://doi.org/10.1088/1755-1315/113/1/012206.
32 Azarian MH and Sutapun W, *Front Mater* **9**:1024977 (2022). https://doi.org/10.3389/fmats.2022.1024977.
33 Schröder R, Pohlit H, Schüler T, Panthöfer M, Unger RE, Frey H *et al.*, *J Mater Chem B* **3**:7079–7089 (2015). https://doi.org/10.1039/C5TB01032B.
34 Unger RE, Stojanovic S, Besch L, Alkildani S, Schröder R, Jung O *et al.*, *Int J Mol Sci* **23**:1196 (2022). https://doi.org/10.3390/ijms23031196.
35 Li X, Yang X, Liu X, He W, Huang Q, Li S *et al.*, *Prog Nat Sci Mater Int* **28**: 598–608 (2018). https://doi.org/10.1016/j.pnsc.2018.09.004.
36 Saveleva MS, Ivanov AN, Chibrikova JA, Abalymov AA, Surmeneva MA, Surmenev RA *et al.*, *Macromol Biosci* **21**:e2100266 (2021). https://doi.org/10.1002/mabi.202100266.
37 Kokubo T and Yamaguchi S, *J Biomed Mater Res A* **107**:968–977 (2019). https://doi.org/10.1002/jbm.a.36620.
38 Ercan B, Oral ÇM and Derya K, *Sakarya Univ J Sci* **23**:129–138 (2019). https://doi.org/10.16984/saufenbilder.433985.
39 Oral ÇM and Ercan B, *Powder Technol* **339**:781–788 (2018). https://doi.org/10.1016/j.powtec.2018.08.066.
40 Khanjani M, Westenberg DJ, Kumar A and Ma H, *ACS Omega* **6**:11988–12003 (2021). https://doi.org/10.1021/acsomega.1c00559.
41 Muljani S, Saputra EA and Sumada K, *Reaktor* **21**:27–34 (2021). https://doi.org/10.14710/reaktor.21.1.27-34.
42 Valkov A, Zinigrad M, Sobolev A and Nisnevitch M, *Int J Mol Sci* **21**:3512 (2020). https://doi.org/10.3390/ijms21103512.
43 Mattiello S, Guzzini A, Del Giudice A, Santulli C, Antonini M, Lupidi G *et al.*, *Polymers* **15**:181 (2022). https://doi.org/10.3390/polym15010181.
44 Abdelrazek EM, Hezma AM, El-Khodary A and Elzayat AM, *Egypt J Basic Appl Sci* **3**:10–15 (2016). https://doi.org/10.1016/j.ejbas.2015.06.001.
45 Leelatawonchai P and Laonapakul T, *Adv Mater Res* **931–932**:370–374 (2014). https://doi.org/10.4028/www.scientific.net/AMR.931-932.370.
46 Zhao X, Lui YS, Choo CKC, Sow WT, Huang CL, Ng KW *et al.*, *Mater Sci Eng C* **49**:746–753 (2015). https://doi.org/10.1016/j.msec.2015.01.084.
47 Cruz-Maya I, Varesano A, Vineis C and Guarino V, *Polymers* **12**:1671 (2020). https://doi.org/10.3390/polym12081671.
48 Sambudi NS, Kim MG and Park SB, *Mater Sci Eng C* **60**:518–525 (2016). https://doi.org/10.1016/j.msec.2015.11.079.
49 Haque AN and Naebe M, *Polymers* **15**:3439 (2023). https://doi.org/10.3390/polym15163439.
50 Lozano-Sánchez LM, Bagudanch I, Sustaita AO, Iturbe-Ek J, Elizalde LE, Garcia-Romeu ML *et al.*, *Polymers* **10**:391 (2018). https://doi.org/10.3390/polym10040391.
51 Feroz N, Muhammad S, Dias G and Alsaiari MA, *J Mol Liq* **350**:118595 (2022). https://doi.org/10.1016/j.molliq.2022.118595.
52 Tohidlou H, Shafiei SS, Abbasi S, Asadi-Eydivand M and Fathi-Roudsari M, *Fibers Polym* **20**:1869–1882 (2019). https://doi.org/10.1007/s12221-019-1262-1.
53 Sani IS, Rezaei M, Khoshfetrat AB and Razzaghi D, *Int J Biol Macromol* **182**:1638–1649 (2021). https://doi.org/10.1016/j.ijbiomac.2021.05.163.
54 Chouzouri G and Xanthos M, *Acta Biomater* **3**:745–756 (2007). https://doi.org/10.1016/j.actbio.2007.01.005.
55 Edwards A, Jarvis D, Hopkins T, Pixley S and Bhattarai N, *J Biomed Mater Res B* **103**:21–30 (2015). https://doi.org/10.1002/jbm.b.33172.

